# Microwave Spectrum, Structure, Dipole Moment and Internal Rotation of Ethanethiol. II. *Gauche* Isomer

Jun NAKAGAWA, Kazunori KUWADA, and Michiro HAYASHI

*Department of Chemistry, Faculty of Science, Hiroshima University, Higashi-sendamachi, Hiroshima 730*

(Received June 2, 1976)

The microwave spectra of *gauche*-ethanethiol and its isotopic species were studied. Most of the observed spectra for the species having the plane of symmetry exhibited doublet structures with large spacings due to the internal rotation of the mercapto group. The $r_s$ structure of the *gauche* isomer was determined from the observed moments of inertia. The *gauche* isomer whose dihedral angle $\tau$(CCSH) is 61°45′±58′ has structural parameters close to those for the *trans* isomer except the angles around the carbon atom in the methylene group. The difference in angle values around the carbon atom in the methylene group between the *trans* and *gauche* isomers can be explained by the 3°7′ tilt of the methylene group towards the lone pair electrons on the sulfur atom. The direction of the dipole moment in the molecule was discussed on the basis of data given by Schmidt and Quade. The potential barrier of the mercapto internal rotation was obtained from splittings of the observed spectra. The Fourier coefficients of this barrier are $V_1=-207\pm67$, $V_2=-386\pm27$, and $V_3=1305\pm20$ cal/mol. The spectra due to the excited methyl and mercapto torsional states were also measured for the *trans* and *gauche* isomers. The potential barrier of the methyl internal rotation for the *trans* isomer was found to be 3260±30 cal/mol from splittings of the spectra due to the first excited methyl torsional state.

In previous paper,[1,2] (referred to as I) reports were given on the microwave spectrum of *trans*-ethanethiol in relation to the $r_s$ structure, dipole moment and the observed microwave spectra of *gauche*-ethanethiol. In the present paper, we deal with the microwave spectrum, $r_s$ structure, and internal rotation of both the mercapto and methyl groups of *gauche*-ethanethiol.

After publication of our papers on the *trans* isomer and rough descriptions of the spectra for the *gauche* isomer, Schmidt and Quade[3] reported an independent study on the microwave spectra of *gauche*-ethanethiol and its four deuterated species. They carried out the analysis of the internal rotation of the mercapto group and the dipole moment assuming a certain structure.

We were working on the same subject for the *gauche* isomer as theirs as a continuation of our work on *trans*-ethanethiol. However, publication of our experimental results was deliberately delayed in order to determine a reliable molecular structure[4] for the *gauche* isomer as well as that for the *trans* isomer and to find the spectra in the excited methyl torsional states both for the *trans* and *gauche* isomers. Wherever their measurements overlap ours, the agreement is very good.

## Exprimental

Normal and deuterated species of ethanethiol were prepared and purified in the same manner as described in I. Two $^{13}C$ species were prepared from the corresponding $^{13}C$ enriched ethyl iodides (90 atom% $^{13}C$, Merck Sharp & Dohme, Canada) by the standard method.[5] The spectra of $^{34}S$ species were measured with a sample containing this species in natural isotopic abundance. Measurements were carried out by the same apparatus and under the same conditions as those in I.

## Microwave Spectra of *Gauche* Isomer

*gauche*-Ethanethiol is a slightly asymmetric prolate top molecule as is *trans*-ethanethiol. Though *a*-, *b*-, and *c*-type transitions are expected for the microwave spectra, *b*-type transitions are actually very weak.

Microwave spectra of *a*- and *c*-types belonging to the *gauche* isomer in the ground state were measured and assignments made for the normal and nine isotopically substituted species of ethanethiol. Observed frequencies with $J\leqq7$ are given in Tables 1 and 2. *s*- and *a*- (*e.g.* *s*-$CH_2DCH_2SH$) stand for the species whose deuterium atoms are situated in the CCS plane and out of the CCS plane, respectively, and -1 and -2 (*e.g.* *a*-$CH_2DCH_2SH$-2) stand for the species whose deuterium atoms are situated on the opposite side and the same side of the CCS plane as the hydrogen atom in the mercapto group, respectively.

The observed spectra for some of the species exhibit doublet structures whose components have identical Stark effects.[1,2]

The normal and nine isotopic species of *gauche*-ethanethiol can be classified into three groups by means of the fine structures of the spectra. Group I($CH_3CH_2SH$, $CH_3CH_2{}^{34}SH$, $^{13}CH_3CH_2SH$, $CH_3{}^{13}CH_2SH$, and *s*-$CH_2DCH_2SH$) consists of the species which have the symmetry plane in the $CH_3CH_2S$ part of the molecule. For Group I, observed *c*-type spectra are doublets with spacings of about 3500 MHz, *a*-type spectra with $K_{-1}=1$ are doublets with spacings of several MHz, and *a*-type spectra with $K_{-1}\neq1$ are singlets. For the $CH_3CH_2$-SD species (Group II), *c*-type spectra are doublets with spacings of about 140 MHz, while *a*-type spectra are singlets. For Group III, in which each species has an isotopically substituted atom situated out of the CCS plane, (*a*-$CH_2DCH_2SH$-1, *a*-$CH_2DCH_2SH$-2, $CH_3CHDSH$-1, and $CH_3CHDSH$-2), spectra are singlets.

For the species belonging to Groups I and II, tunnelling effect between two equivalent *gauche* minima in the internal rotation potential function of the mercapto group produces two different energy states (referred to as the + and − states). The + and − states indicate the symmetric and antisymmetric states with respect to the mercapto internal rotation angle, respectively. The energy difference between the + and − states for the SH group is greater than that for the SD group since the reduced moment of inertia around the internal rotation axis for the SD group is greater

Table 1. Observed frequencies of group I and II species of *gauche*-ethanethiol[a] (MHz)

| Transition[b] | $CH_3CH_2SH$ | $CH_3CH_2SD$ | *s*-$CH_2DCH_2SH$ | $CH_3CH_2{}^{34}SH$ | $^{13}CH_3CH_2SH$ | $CH_3{}^{13}CH_2SH$ |
|---|---|---|---|---|---|---|
| $1_{01}\leftarrow 0_{00}{}^{++}_{--}$ | 10141.07( 10) | 9958.84( 16) | 9489.97( 13) | 9920.24( 6) | 9844.82( −4) | 10087.97( 6) |
| $2_{02}\leftarrow 1_{01}{}^{++}_{--}$ | 20275.47( −7) | 19911.04( −1) | 18914.87( −2) | 19834.47( −2) | 19683.78( −8) | 20168.67(−10) |
| $2_{12}\leftarrow 1_{11}{}^{++}_{--}$ | 19832.99( 3)<br>19836.33(−27) | 19496.00( 4) | 18528.69( 17)<br>18530.38( −5) | 19409.88( 11)<br>19412.97( −1) | 19260.50( −2)<br>19263.38(−18) | 19710.80( −8)<br>19715.72(−22) |
| $2_{11}\leftarrow 1_{10}{}^{++}_{--}$ | 20727.77( 50)<br>20730.83( −8) | 20338.84( 7) | 19309.39( 44)<br>19310.84( −1) | 20267.93( 21)<br>20270.63(−31) | 20116.28( 41)<br>20118.90( −1) | 20636.00( 30)<br>20640.61(−15) |
| $3_{03}\leftarrow 2_{02}{}^{++}_{--}$ | 30396.99(−43) | 29850.64(−15) | 28359.91(−45) | ——[c] | 29511.19( 4) | 30235.33(−23) |
| $3_{13}\leftarrow 2_{12}{}^{++}_{--}$ | 29745.06(−17)<br>29736.75( −1) | 29239.96( −6) | 27789.32(−28)<br>27781.13( −3) | 29110.56(−22)<br>29102.16(−31) | 28886.65(−27)<br>28878.63(−14) | 30966.87( 7)<br>30956.66(−30) |
| $3_{12}\leftarrow 2_{11}{}^{++}_{--}$ | 31101.19( 14)<br>31092.52( −5) | 30504.02(−16) | 28971.99( 8)<br>28963.54( 7) | 30411.19( −7)<br>30402.44(−51) | 30183.09( 3)<br>30174.59(−32) | 29561.49(−21)<br>29551.76(−10) |
| $3_{22}\leftarrow 2_{21}{}^{++}_{--}$ | 30423.63( 65) | 29876.33( 28) | 28379.94( 35) | 29761.26( 66) | 29535.10( 45) | 30264.28( 45) |
| $3_{21}\leftarrow 2_{20}{}^{++}_{--}$ | 30448.16(−23) | 29901.17(−13) | 28398.62( −2) | 29783.78(−12) | 29557.77(−15) | 30291.72( −9) |
| $1_{10}\leftarrow 0_{00}{}^{+-}_{-+}$ | 32287.96( 4)<br>——[c] | 31184.15( 46)<br>31324.48( 14) | | | | |
| $1_{11}\leftarrow 1_{01}{}^{+-}_{-+}$ | 21697.94(−46)<br>25206.36( 9) | 20803.25(−35)<br>20944.11(−14) | 21989.18(−31)<br>25569.18( 10) | 21804.58( 87)<br>25264.92( −2) | 21660.58(−30)<br>25146.83( 19) | 21086.01(−22)<br>24534.46( 18) |
| $2_{12}\leftarrow 2_{02}{}^{+-}_{-+}$ | 21255.73( −9)<br>24767.49( 16) | 20388.32(−19)<br>20529.11( −6) | 21602.99(−13)<br>25184.58( −3) | 21378.33(−65)<br>24843.29(−13) | 21237.38(−16)<br>24726.32( −2) | 20628.15(−19)<br>24081.47( 2) |
| $3_{13}\leftarrow 3_{03}{}^{+-}_{-+}$ | 20603.87( 15)<br>24106.74( −2) | 19777.71( −3)<br>19918.41( 1) | 21032.42( 6)<br>24605.51( 10) | 20752.16(−52)<br>24208.97( 15) | 20613.44( 13)<br>24094.01( 5) | 19954.55( 7)<br>23397.74( 0) |
| $4_{14}\leftarrow 4_{04}{}^{+-}_{-+}$ | 19756.94( 40)<br>23260.82(−23) | 18985.68( 12)<br>19126.26( 5) | 20288.39( 37)<br>23863.88(−17) | 19938.35( 31)<br>23395.86( 2) | 19801.74( 33)<br>23283.55(−22) | 19080.91( 34)<br>22524.90(−21) |

Additional Observed Frequencies of the Normal Species ($CH_3CH_2SH$).

| | | | | | |
|---|---|---|---|---|---|
| $4_{04}\leftarrow 3_{03}{}^{++}_{--}$ | 40499.40(−60) | $4_{13}\leftarrow 3_{12}{}^{++}_{--}$ | 41448.46( 61)<br>41449.06(−27) | $4_{22}\leftarrow 3_{21}{}^{++}_{--}$ | 40622.43( 12) |
| $4_{14}\leftarrow 3_{13}{}^{++}_{--}$ | 39652.32(−51)<br>39653.65(−65) | $4_{23}\leftarrow 3_{22}{}^{++}_{--}$ | 40559.34( 25) | $4_{32}\leftarrow 3_{31}{}^{++}_{--}$<br>$4_{31}\leftarrow 3_{30}{}^{++}_{--}$ | ( 18)<br>40576.67<br>(−16) |

a) Observed frequencies of the species whose $CH_3CH_2S$ part of the molecule has the plane of symmetry. Figures in parentheses indicate the differences between the observed and calculated frequencies.
b) − + indicates the transition from the + state to the − state and so on.
c) Overlapped with the other spectra.

Table 2. Observed frequencies of group III species of *gauche*-ethanethiol[a] (MHz)

| Transition | *a*-$CH_2DCH_2SH$-1 | *a*-$CH_2DCH_2SH$-2 | $CH_3CHDSH$-1 | $CH_3CHDSH$-2 |
|---|---|---|---|---|
| $1_{01}\leftarrow 0_{00}$ | 9787.90( 6) | 9779.36( 12) | 9988.38( −3) | 9979.41( −5) |
| $2_{02}\leftarrow 1_{01}$ | 19569.18( 0) | 19551.40( −2) | 19967.48( 7) | 19950.22( −7) |
| $2_{12}\leftarrow 1_{11}$ | 19148.99( −5) | 19112.53(−14) | 19473.71(−23) | 19479.10( −9) |
| $2_{11}\leftarrow 1_{10}$ | 20002.16( 1) | 20004.21( 7) | 20479.63( 9) | 20438.54( 11) |
| $3_{03}\leftarrow 2_{02}$ | 29337.30(−23) | 29309.35(−14) | 29927.47(−12) | 29903.64(−24) |
| $3_{13}\leftarrow 2_{12}$ | 28719.12(−24) | 28664.52( 2) | 29204.65(−26) | 29213.13(−10) |
| $3_{12}\leftarrow 2_{11}$ | 29999.02( 6) | 30001.74( 11) | 30713.33( 12) | 30652.19( 21) |
| $3_{22}\leftarrow 2_{21}$ | 29363.35( 18) | 29337.30(−13) | 29965.14( 25) | 29938.15( 22) |
| $3_{21}\leftarrow 2_{20}$ | 29389.07( 25) | 29365.54( 16) | 30002.22( 3) | 29971.89( −9) |
| $1_{10}\leftarrow 0_{00}$ | 31276.34( 8) | 31321.32( 4) | 30559.62( 12) | 30473.37( 12) |
| $1_{11}\leftarrow 1_{01}$ | 21061.92( 6) | 21096.25( −5) | 20068.25( −4) | 20014.31( 14) |
| $2_{12}\leftarrow 2_{02}$ | 20641.66( −6) | 20657.59( 4) | 19574.79( −2) | 19543.03( −4) |
| $3_{13}\leftarrow 3_{03}$ | 20023.45(−10) | 20012.48( −8) | 18851.99(−14) | 18852.25(−17) |
| $4_{14}\leftarrow 4_{04}$ | 19221.73(−12) | 19177.13( 3) | 17921.33( 4) | 17961.37( −8) |
| $5_{15}\leftarrow 5_{05}$ | 18256.09( 22) | 18172.23( 7) | 16809.99(−23) | 16895.38(−28) |
| $6_{16}\leftarrow 6_{06}$ | | | 15553.26( 5) | 15686.46( 1) |
| $7_{17}\leftarrow 7_{07}$ | | | 14190.08( 21) | 14370.55( 32) |

a) Observed frequencies of the species whose $CH_3CH_2S$ part of the molecule has no plane of symmetry. Figures in parentheses indicate the difference between the observed and calculated frequencies.

TABLE 3. OBSERVED ROTATIONAL CONSTANTS (MHz) OF *gauche*-ETHANETHIOL[a)]

| Species | $A$ | $B$ | $C$ | $D_J \times 10^{3}$ [b)] | $\Delta\nu$[c)] | $D_{\pm}$[d)] |
|---|---|---|---|---|---|---|
| $CH_3CH_2SH$ | 28747.09(50) | 5294.78(12) | 4846.18(12) | —— | 1753.84(29) | 12.43(37) |
| $CH_3CH_2SD$ | 26063.97(21) | 5190.04( 5) | 4768.64( 5) | —— | 70.33(14) | —— |
| $CH_3CH_2{}^{34}SH$ | 28709.50(62) | 5175.20(15) | 4744.98(15) | —— | 1730.53(35) | 12.07(46) |
| $^{13}CH_3CH_2SH$ | 28540.59(36) | 5136.85( 9) | 4708.01( 9) | —— | 1742.79(21) | 11.93(28) |
| $CH_3{}^{13}CH_2SH$ | 28056.43(36) | 5276.21( 9) | 4811.70( 9) | —— | 1723.91(21) | 13.32(24) |
| *s*-$CH_2DCH_2SH$ | 28704.62(38) | 4925.35( 9) | 4534.49( 9) | —— | 1789.73(23) | 10.76(27) |
| *a*-$CH_2DCH_2SH$-1 | 26169.06(72) | 5107.21(13) | 4680.65(14) | 3.7(65) | —— | —— |
| *a*-$CH_2DCH_2SH$-2 | 26208.79(48) | 5112.49( 9) | 4666.76(10) | 3.0(43) | —— | —— |
| $CH_3CHDSH$-1 | 25313.90(54) | 5245.62( 8) | 4742.81( 9) | 3.6(60) | —— | —— |
| $CH_3CHDSH$-2 | 25243.72(60) | 5229.55( 9) | 4749.93(10) | 4.8(68) | —— | —— |

a) Figures in parentheses indicate the uncertainty attached to the last significant figures calculated from 2.5 times the standard deviations. b) $10^3$ times the coefficient of the $[J(J+1)]^2$ term in the centrifugal distortion formula in MHz. For the first six species, this term is neglected in the determination of the rotational constants. In Table 2 of the previous paper on the *trans* isomer (Ref. 2), signs of the corresponding $D_J$ values were mistyped, that is, $-4.68$ in that table should read 4.68 and so on. c) Energy difference between the + and − states. d) Coefficient of $(P_xP_y+P_yP_x)$ term in Eq. 3c.

than for the SH group.

From group-theoretical considerations, the selection rules governing transitions between the rotational energy levels belonging to the + and − states are + ↔ + and − ↔ − for *a*-type transitions and + ↔ − for *c*-type transitions.

In order to obtain the rotational constants from the observed frequencies for the species belonging to Groups I and II, we must consider the effective Hamiltonian which includes not only the rigid rotor terms of the + and − states but also cross terms between the + and − states. The rotational constants obtained are given in Table 3. It is found that the rotational constants of the + and − states are essentially equal within experimental error for the species belonging to Groups I and II.

For the species belonging to Group III, splittings of the + and − states cannot occur because there are no equivalent *gauche* forms. Although the *a*-$CH_2D$-$CH_2SH$ species has two equivalent *gauche* forms, tunnelling effect between these two conformers occurs through the internal rotation potential of not only the mercapto group but also the methyl group. Splittings of the + and − states are negligibly small. The rotational constatnts were obtained by a least squares analysis from all the observed frequencies so as to fit in with a modified rigid rotor expression which includes only the $D_J[J(J+1)]^2$ term of the centrifugal distortion formula. The rotational constants are given in Table 3.

## Analysis of Doublet Structures of the Observed Spectra for the *Gauche* Isomer

Analysis of doublet structures of the observed spectra is necessary for the species belonging to Groups I and II. In order to derive the Hamiltonian for the coupling problem of overall rotation and internal rotation of the mercapto group, the coordinate system for the species belonging to Groups I and II is so chosen that the z-axis is parallel to the mercapto internal rotation axis, the y-axis is in the symmetry plane, and the x-axis is perpendicular to the symmetry plane. The Hamiltonian concerning overall and internal rotation is then written as the sum of the overall rotation, internal rotation, and overall-internal rotation interaction terms:[6)]

$$H = H_{\text{rot}} + H_{\text{int}} + H_{\text{rot-int}}, \tag{1}$$

$$\begin{aligned} H_{\text{rot}} = {} & \sum \mu_{xx}^{(n)} \cos n\alpha \cdot P_x^2 + \sum \mu_{yy}^{(n)} \cos n\alpha \cdot P_y^2 \\ & + \sum \mu_{zz}^{(n)} \cos n\alpha \cdot P_z^2 + \sum \mu_{yz}^{(n)} \cos n\alpha \cdot (P_yP_z + P_zP_y) \\ & + \sum \mu_{xz}^{(n)} \sin n\alpha \cdot (P_xP_z + P_zP_x) \\ & + \sum \mu_{xy}^{(n)} \sin n\alpha \cdot (P_xP_y + P_yP_x), \end{aligned} \tag{1a}$$

$$\begin{aligned} H_{\text{int}} = {} & \sum \mu_{\alpha}^{(n)} (p_\alpha^2 \cos n\alpha + \cos n\alpha \cdot p_\alpha^2) \\ & + \sum \frac{V_n}{2} (1 - \cos n\alpha), \end{aligned} \tag{1b}$$

$$\begin{aligned} H_{\text{rot-int}} = {} & \sum \mu_{\alpha x}^{(n)} (p_\alpha \sin n\alpha + \sin n\alpha \cdot p_\alpha) P_x \\ & + \sum \mu_{\alpha y}^{(n)} (p_\alpha \cos n\alpha + \cos n\alpha \cdot p_\alpha) P_y \\ & + \sum \mu_{\alpha z}^{(n)} (p_\alpha \cos n\alpha + \cos n\alpha \cdot p_\alpha) P_z, \end{aligned} \tag{1c}$$

where $\mu_{gg'}^{(n)}$, represents the $n$-th Fourier coefficient of the $g,g'$-th element of the reciprocal inertia tensor, $\alpha$ denotes the mercapto internal rotation angle, and $P_x$, $P_y$, $P_z$, and $p_\alpha$ represent x, y, and z components of the total angular momentum and the mercapto internal rotational angular momentum, respectively.

Assuming that the wave functions for the Hamiltonian (1) can be written as the products of overall and internal rotation wave functions and that internal rotation wave functions are obtained as the eigenfunctions of Eq. 1b, the effective Hamiltonian for the overall rotation is reduced to the following formulas.

$$\begin{aligned} \langle + |H| + \rangle = {} & A'_+P_z^2 + B'_+P_y^2 + C'_+P_x^2 + F'_+(P_yP_z + P_zP_y) \\ & + M'_+P_x, \end{aligned} \tag{2a}$$

$$\begin{aligned} \langle - |H| - \rangle = {} & A'_-P_z^2 + B'_-P_y^2 + C'_-P_x^2 + F'_-(P_yP_z + P_zP_y) \\ & + M'_+P_x + \Delta\nu, \end{aligned} \tag{2b}$$

$$\begin{aligned} \langle + |H| - \rangle = {} & D'_{\pm}(P_xP_y + P_yP_x) + E'_{\pm}(P_xP_z + P_zP_x) \\ & + N'_{\pm}P_y + Q'_{\pm}P_z, \end{aligned} \tag{2c}$$

where $\Delta\nu$ denotes the pure internal rotational energy difference between the + and − states. Coefficients $A'_+$, *etc.* are obtained as the matrix elements of the cor-

responding operators between the wave functions of + and +, or − and −, or + and − states. The cross term in Eq. 2c occurs from the odd functions of $\alpha$, $\sin n\alpha$ and $(p_\alpha \cdot \cos n\alpha + \cos n\alpha \cdot p_\alpha)$, in Eq. 1.

After a suitable rotation about the x-axis is carried out, it is possible that Eqs. 2a and 2b are reduced to formulas containing no $(P_yP_z+P_zP_y)$ term. Furthermore, the $P_x$ terms in Eqs. 2a and 2b can be neglected, since these terms contribute to the off-diagonal matrix elements, whose $K_{-1}$ values are not equal. Thus the effective Hamiltonians are written as

$$\langle + |H| + \rangle = A_+P_z^2 + B_+P_y^2 + C_+P_x^2, \quad (3a)$$

$$\langle - |H| - \rangle = A_-P_z^2 + B_-P_y^2 + C_-P_x^2 + \Delta\nu \quad (3b)$$

$$\langle + |H| - \rangle = D_\pm(P_xP_y+P_yP_x) + E_\pm(P_xP_z+P_zP_x) + N_\pm P_y + Q_\pm P_z \quad (3c)$$

Taking account of the selection rules of *a*- and *c*-type transitions, it can be concluded that doublet structures of *a*-type transitions are due to the difference in the rotational constants of the + and − states or/and the cross terms of Eq. 3c, while doublet structures of *c*-type transitions arise mainly from the energy difference $\Delta\nu$ between the + and − states.

*Group I.* Since observed *a*-type transitions are singlets except $K_{-1}=1$ transitions, the rotational constants of the + and − states are regarded to be approximately equal to each other. Doublet structures of $K_{-1}=1$ transitions are due to the cross terms in Eq. 3c.

For the normal species, *a*-type $J=2\rightarrow3$ transitions with $K_{-1}=1$ have the largest splittings of all the *a*-type transitions.

This is understandable if the $2_{11}$ level of the + state is accidentally degenerate with the $2_{12}$ level of the − state (referred to as $2_{11}^+$ and $2_{12}^-$). Furthermore, the fact that the splittings of $J=1\rightarrow2$ transitions are greater than those of $J=3\rightarrow4$ transitions indicates that the

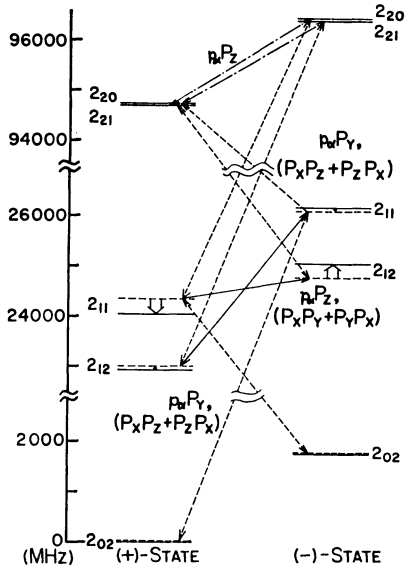


Fig. 1. The interaction scheme between the + and − states for $J=2$ levels of the normal species. Solid and dotted lines indicate perturbed and unperturbed levels, respectively.

$2_{11}^+$ level is slightly lower than the $2_{12}^-$ level.

The interaction scheme of the cross terms are shown for the normal species in Fig. 1. Since the molecule is a nearly prolate symmetric top, the $P_z$ term connects two levels with the same $K_{-1}$, while the $(P_xP_y+P_yP_x)$ term connects two levels whose $K_{-1}$ values differ by 2 from each other except $K_{-1}=1$ levels. However, the observed spectra show doublet structures only in the case of $K_{-1}=1$ transitions. Thus we cannot determine the contributions due to the $P_z$ and $(P_xP_y+P_yP_x)$ terms independently. The determination might be possible if the transitions with $J=8$ or 9 are available, since the levels with $J=8$ or 9 would exhibit the degeneracy for $K_{-1}=2$ levels which is affected by the $P_z$ term most sensitively. However, the corresponding transitions are expected out of our observable frequency region.

The $(P_xP_z+P_zP_x)$ and $P_y$ terms affect the splittings only by a small amount, since the energy difference of the levels which perturb each other through these terms is ten times larger than those in the case of $P_z$ connections so that the corresponding levels of the + and − states are equally pushed up or down. Schmidt and Quade[3] determined the coefficient of the $(P_xP_z+P_zP_x)$ term neglecting the $P_y$ term but the error of this coefficient would be fairly large. We have analyzed the doublet structures by taking account of only the $(P_xP_y+P_yP_x)$ term of Eq. 3c.

For the *c*-type transitions, splittings are about twice the energy difference between the + and − states, *i.e.*, $2\Delta\nu$. The assignments of the *c*-type *Q* branch transitions were made taking account of the roughly estimated value of $\Delta\nu$ from the *a*-type transitions. A least squares analysis was carried out using rotational constants *A*, *B*, *C*, energy difference $\Delta\nu$, and the coefficient of the cross term $D_\pm$, as parameters. Centrifugal distortion effect was neglected since relatively low *J* transitions were used.

As is shown in Table 8 for the normal species, if a suitable choice of the components of the doublets is made, the observed *a*-type transition frequencies can be fitted with the rigid rotor expression giving the rotational constants *B* and *C* which are equal to the rotational constants obtained by the above procedures within the experimental error. This is explained as follows.

Since the rotational constants for the + and − states are approximately equal to each other, the frequencies of a given *a*-type transition for the + and − states are equal to each other if all the coupling terms are negligible. However, for the transitions with $K_{-1}=1$, the energy difference between the + and − states makes pairs of energy levels such as $(1_{10}^+, 1_{11}^-)$, $(2_{11}^+, 2_{12}^-)$, and $(3_{12}^+, 3_{13}^-)$ to be in an accidental degeneracy and the coupling term $(P_xP_y+P_yP_x)$ makes a level in a pair shift to the upper side and the other to the lower side. The frequencies of the transitions containing these levels shift from the original values. On the other hand, the coupling term makes little influence on pairs of energy levels such as $(1_{10}^-, 1_{11}^+)$, $(2_{11}^-, 2_{12}^+)$, and $(3_{12}^-, 3_{13}^+)$ which are not in degeneracy. The frequencies of the transitions containing these levels remain unchanged and they can be fitted with the rigid rotor expression as well as those of the transitions with $K_{-1}=0$ or 2.

*Group II.* For this group, there are no splittings for the *a*-type transitions, all the observed *c*-type transitions having splittings of about 140 MHz. The analysis of the observed spectra was carried out by a least squares technique using rotational constants and energy difference $\Delta v$ as parameters neglecting centrifugal distortion contributions.

### $r_s$ Structure

Our present data are sufficient to determine the $r_s$ structure for the *gauche* isomer by the substitutuion method. However, there are several atoms situated close to one of the principal axes for the *gauche* isomer. Solutions of the Kraitchman equations are not reliable for the coordinates having small absolute values for these atoms. These "bad" coordinates must be calculated from other reliable coordinates either with the aid of the first moment equations or by some assumptions on the structure.

There are five so-called "bad" coordinates for the *gauche* isomer: 1) $x_c$ coodinates of the carbon atoms in the methylene and methyl groups, 2) $x_b$ and $x_c$ coordinates of the hydrogen atom labeled by $H_s$ in the methyl group, and 3) $x_c$ coodinate of the sulfur atom.

We have three first moment equations and three inertia products which should be zero in the principal axis system. Then, if desirable, some of the five "bad" coordinates can be obtained from these six relations. However, use of the inertia products makes the error of the calculated coordinates greater in general and some of three first moment equations will be useful for confirmation of the results. The following assumptions on the structure were made for the calculation of the "bad" coordinates.

The most reasonable assumptions for $x_c$ coordinates of the carbon atoms in the methylene and methyl groups are probably $r(CH^1)=r(CH^2)$ and $r(CH_a^1)=r(CH_a^2)$, since these bond lengths are equal to each other from the symmetry for the *trans* isomer. For $x_b$ and $x_c$ coordinates of the $H_s$ atom in the methyl group, assumptions $r(CH_s)=r(CH_a^1)=r(CH_a^2)$ and $r(H_sH_a^1)=r(H_sH_a^2)$ are acceptable, since $r(CH_s)$ and $r(CH_a)$ for the *trans* isomer are essentially equal to each other within experimental error. The name of each atom is shown in Fig. 2.

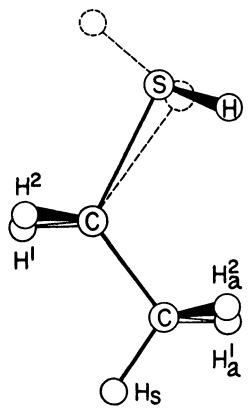


Fig. 2. Symbols of atoms in *gauche*-ethanethiol.

The $x_c$ coordinate of the sulfur atom was solved by use of the first moment equation. The coordinates obtained are given in Table 5 where the calculated two first moments and three inertia products are also given for confirmation of the adequacy of the assumptions. Deviations of the calculated moments of inertia from the observed are also given in Table 4, for all the species. The root mean square deviation for thirty moments of inertia is 0.3938 amu Å which is satisfactorily small.

Structural parameters calculated from atom coordinates are given in Table 6, in comparison with those for the *trans* isomer.[2]

Despite many "bad" coordinates, the structural parameters for the *gauche* isomer are reliable in a similar extent to those for the *trans* isomer. Structural parameters of the CSH and $CH_3C$ parts of the *gauche* isomer are essentially equal to those of the *trans* isomer, except slightly longer $r$(SH) and shorter $r$(CS) values (Table 6). The dihedral angle $\tau$(CCSH) for the *gauche* isomer can also be determined satisfactorily.

Significant discrepancies are found in the six angles around the carbon atom in the methylene group. This was expected in I from the anomalous smallness of $\alpha$(CCS) in the *trans* isomer. This was explained by considering the tilt of the ethyl group towards the lone pair electrons on the sulfur atom in a similar manner to the case of the methyl group in methanethiol. The

TABLE 4. MOMENTS OF INERTIA (amu Å$^2$)[a]

| Species | $I_a$ | $\delta I_a$[b] | $I_b$ | $\delta I_b$[b] | $I_c$ | $\delta I_c$[b] | $P_c$[c] | $\Delta P_c$[d] |
|---|---|---|---|---|---|---|---|---|
| $CH_3CH_2SH$ | 17.5801 (3) | 0.0627 | 95.4480 (22) | 0.4812 | 104.2834 (26) | 0.4831 | 4.3723 (17) | —— |
| $CH_3CH_2SD$ | 19.3898 (2) | 0.0667 | 97.3742 ( 9) | 0.4910 | 105.9791 (11) | 0.4809 | 5.3925 ( 7) | 1.0202 (18) |
| $CH_3CH_2{}^{34}SH$ | 17.6031 (4) | 0.0624 | 97.6534 (28) | 0.4870 | 106.5075 (34) | 0.4907 | 4.3745 (22) | 0.0022 (28) |
| $^{13}CH_3CH_2SH$ | 17.7073 (2) | 0.0630 | 98.3825 (17) | 0.4756 | 107.3439 (21) | 0.4786 | 4.3729 (13) | 0.0006 (22) |
| $CH_3{}^{13}CH_2SH$ | 17.9936 (2) | 0.0595 | 95.7839 (16) | 0.4771 | 105.0307 (20) | 0.4793 | 4.3734 (13) | 0.0011 (21) |
| *s*-$CH_2DCH_2SH$ | 17.6061 (2) | 0.0692 | 102.6071 (19) | 0.4806 | 111.4516 (22) | 0.4727 | 4.3808 (15) | 0.0085 (22) |
| *a*-$CH_2DCH_2SH$-1 | 19.3119 (4) | 0.0653 | 98.9531 (23) | 0.4694 | 107.9718 (30) | 0.4876 | 5.1466 (19) | 0.7743 (26) |
| *a*-$CH_2DCH_2SH$-2 | 19.2827 (3) | 0.0642 | 98.8509 (19) | 0.4838 | 108.2929 (26) | 0.4747 | 4.9203 (16) | 0.5480 (23) |
| $CH_3CHDSH$-1 | 19.9644 (4) | 0.0596 | 96.3425 (15) | 0.4862 | 106.5562 (20) | 0.4684 | 4.8753 (13) | 0.5030 (21) |
| $CH_3CHDSH$-2 | 20.0199 (5) | 0.0593 | 96.6385 (17) | 0.4690 | 106.3965 (22) | 0.4862 | 5.1309 (14) | 0.7586 (22) |

a) Figures in parentheses indicate the uncertainty attached to the last significant figures calculated from 2.5 times the standard deviations. b) $I_{obsd}-I_{calcd}$. $I_{calcd}$ is calculated from the coordinates listed in Table 5. c) $P_c=(I_a+I_b-I_c)/2$. d) $\Delta P_c=P_c(\text{isotopic})-P_c(\text{parent})$.

Table 5. Atom coordinates[a] and check calculations of *gauche*-ethanethiol

| Atom | Group | $x_a$ | $x_b$ | $x_c$ | Assumption used |
|---|---|---|---|---|---|
| Atom Coordinates (Å) | | | | | |
| H | SH | −0.9460(24) | −0.8446( 25) | 1.0647(24) | |
| S | | −1.0672(17) | −0.1053(176) | −0.0414(17) | $x_c$ from $\sum_i m_i(x_c)_i=0$ |
| C | $CH_2$ | 0.5807(46) | 0.6476( 42) | 0.0519(29) | $x_c$ from $r(CH^1)=r(CH^2)$ |
| $H^1$ | $CH_2$ | 0.6193(42) | 1.3417( 19) | −0.7866(41) | |
| $H^2$ | $CH_2$ | 0.6503(42) | 1.2491( 21) | 0.9572(35) | |
| C | $CH_3$ | 1.7221(16) | −0.3647( 78) | −0.0317(33) | $x_c$ from $r(CH_a^1)=r(CH_a^2)$ |
| $H_s$ | $CH_3$ | 2.6864(11) | 0.1450(128) | −0.0201(35) | $x_b$, $x_c$ from $r(CH_s)=r(CH_a)$, $r(H_sH_a^1)=r(H_sH_a^2)$ |
| $H_a^1$ | $CH_3$ | 1.6428(19) | −0.9555( 32) | −0.9453(39) | |
| $H_a^2$ | $CH_3$ | 1.6798(17) | −1.0647( 27) | 0.8038(43) | |

| Inertia tensor for the normal species | | | |
|---|---|---|---|
| $\sum m_i(x_g)_i$(amu Å) g = | a | b | c |
| | −0.1035 | −0.1012 | 0 (assumed) |

| (amu Å²) | $I_a$ | $I_b$ | $I_c$ | $I_{ab}$ | $I_{bc}$ | $I_{ac}$ |
|---|---|---|---|---|---|---|
| Obsd | 17.5801 | 95.4480 | 104.2834 | 0 | 0 | 0 |
| Calctd | 17.5174 | 94.9668 | 103.8003 | −0.0375 | 0.0195 | 0.0389 |

RMS[b] for ten isotopic species used……0.3938 (amu Å²)

a) Figures in parentheses indicate 99% reliability intervals attached to the last significant figures. b) Root mean square deviation of the observed-calculated moments of inertia for all the isotopic species used.

Table 6. Structural parameters of ethanethiol

| Group | Parameter | By the present authors[a] | | By Schmidt *et al.*[c] | |
|---|---|---|---|---|---|
| | | *gauche* | *trans*[b] | *gauche* | *trans* |
| CSH | $r$(SH) Å | 1.336(0.010) | 1.322(0.006) | 1.328 | 1.328 |
| | $r$(SC) Å | 1.814(0.009) | 1.820(0.005) | 1.829 | 1.829 |
| | $\alpha$(HSC) | 96°( 34′) | 96°13′( 23′) | 95°14′ | 95°14′ |
| $CCH_2S$ | $r$(CH) Å | 1.089(0.005) | 1.090(0.003) | 1.088 | 1.088 |
| | $r$(CC) Å | 1.528(0.007) | 1.529(0.006) | 1.530 | 1.530 |
| | $\alpha$(CCS) | 113°37′ (29′) | 108°34′ (19′) | (113°16′) | (108°33′) |
| | $\alpha$(HCH) | 106°35′ (36′) | 108°54′ (22′) | (107°19′) | (107°14′) |
| | $\alpha(H^1CC)$ | 110°42′ (43′) | 110°14′ (33′) | 109°34′ | 109°34′ |
| | $\alpha(H^2CC)$ | 111°19′ (42′) | | | |
| | $\alpha(H^1CS)$ | 104°53′ (57′) | 109°26′ (30′) | (106° 7′) (110°48′) | (110°55′) |
| | $\alpha(H^2CS)$ | 109°16′ (56′) | | | |
| $CH_3C$ | $r(CH_s)$ Å | 1.091(0.007) | 1.095(0.006) | 1.093 | 1.093 |
| | $r(CH_a)$ Å | | 1.092(0.006) | | |
| | $\alpha(CCH_s)$ | 110°30′ (40′) | 109°40′ (34′) | 109°42′ | 109°42′ |
| | $\alpha(CCH_a)$ | 110°37′ (38′) | 110°35′ (29′) | | |
| | $\alpha(H_sCH_a)$ | 109° 2′ (60′) | 108°35′ (49′) | (109°14′) | (109°14′) |
| | $\alpha(H_aCH_a)$ | 106°55′ (43′) | 108° 7′ (33′) | | |
| Dihedral angle | $\tau$(CCSH) | 61°45′ (58′) | 180° | (60°) | 180° |
| Unperturbed | $\alpha$(CCS)[d] | 111°55′ | | 111°43′ | |
| Tilt angle for the $CH_2$ group[d] | | 3° 7′ | | 3°10′ | |

a) Figures in parentheses indicate 99% reliability intervals. Structural parameters for the *gauche* isomer were obtained by the following assumptions. $r(CH^1)=r(CH^2)$ for $CH_2$; $r(CH_a^1)=r(CH_a^2)=r(CH_s)$, $\alpha(CCH_a^1)=\alpha(CCH_a^2)$, $\alpha(H_sCH_a^1)=\alpha(H_sCH_a^2)$ for $CH_3$. b) Quoted from (Ref. 2). c) The proposed structure by Schmidt and Quade (Ref. 3). Figures in parentheses indicate the parameters derived from their parameters. The dihedral angle for the *gauche* isomer is defined as the dihedral angle around the internal rotation axis of the SH group and is not equal to our definition. d) See text.

present structural data for the *gauche* isomer are useful for the explanation.

Let us assume that 1) the methylene group is tilted $\delta°$ towords lone pair electrons on the sulfur atom, 2) the internal rotation axis of the mercapto group does not always coincide with the CS bond, 3) the dihedral angle is defined as that around the internal rotation axis of the mercapto group and is 180° for the *trans* isomer and $\tau°$ for the *gauche* isomer, and 4) $\alpha$(HCH) and $\alpha$(HCC) angles remain unchanged between the *trans* and the *gauche* isomers.

From these assumptions, the following relations can be derived approximately.

For the *trans* isomer,

$$\alpha(\mathrm{CCS})_{trans} = \beta - \gamma \quad (4)$$

$$\alpha(\mathrm{SCH})_{trans} = \gamma + \delta\cos\omega \quad (5)$$

For the *gauche* isomer,

$$\alpha(\mathrm{CCS})_{gauche} = \beta + \delta\cos\tau \quad (6)$$

$$\alpha(\mathrm{SCH^1})_{gauche} = \gamma - \delta\cos(\tau-\omega) \quad (7)$$

$$\alpha(\mathrm{SCH^2})_{gauche} = \gamma - \delta\cos(\tau+\omega) \quad (8)$$

where $\omega$ is the dihedral angle between the symmetry plane and the plane containing the CH bond and the internal rotation axis, and $\beta$ and $\gamma$ indicate the angles made by $r$(CC) and $r$(CH) against the internal rotation axis, respectively, *viz.*, the hypothetical unperturbed $\alpha$(CCS) and $\alpha$(SCH) angles which are free from the influence of the tilt and are common to the *trans* and *gauche* isomers.

In order to evaluate $\delta$, $\beta$, and $\gamma$ values from the relations (4)—(8), we must know the values of $\tau$ and $\omega$, where $\omega$ is a function of $\alpha$(HCH) and $\gamma$. Since the values of $\tau$ and $\omega$ are not far from 60°, it is reasonable as a first approximation to calculate the $\gamma$ value with 60° for both the $\tau$ and $\delta$ values. The value $\gamma$=107°52′ is obtained. Though $\alpha$(HCH) values for the *trans* and *gauche* isomers are not equal to each other beyond experimental error in contrast with the assumption 4), the average (107°45′) of the observed $\alpha$(HCH) values for the two isomers is taken as the value in the evaluation of the $\omega$ angle. $\omega$=57°57′ is obtained using $\gamma$=107°52′ and $\alpha$(HCH)=107°45′. Though the experimentally obtained dihedral angle (61°45′) is actually the one defined around the CS bond, the value is taken as the $\tau$ value in the above relations as an approximation. In the calculation, because of experimental error, choice of three relations from the five gives slightly different values of $\delta$, $\beta$, and $\gamma$. The average values for the different choices are $\delta$=3°7′, $\beta$=111°55′, and $\gamma$=107°50′.

The $\alpha$(HCC) value 110°45′ was obtained, which is in good agreement with the average (110°37′) of the experimentally obtained $\alpha$(HCC) values for the two isomers.

It is interesting that the hypothetical unperturbed $\alpha$(CCS) (=$\beta$) is close to $\alpha$(CCC) in propane (112°24′)[7] and the tilt angle (=$\delta$) is slightly larger than that of the methyl groups in methanethiol[8] and dimethyl sulfide[9] (2°30′). The tilt of the methylene group indicates that the internal rotation axis of the mercapto group does not coincide with the CS bond, a line from the carbon atom in the methylene group to the mercapto group making an angle of 3°7′ with the CS bond.

Schmidt and Quade[3] proposed a structure for ethanethiol. It was obtained so as to fit the calculated moments of inertia with those observed for four species of the *trans* isomer and five species of the *gauche* isomer.

For the structures of the two isomers, they took thirteen structural parameters, some of which have different definitions from ours. They assumed that 1) change in the structure from the *trans* to the *gauche* isomer has been explained solely in terms of the orientation of the mercapto group, 2) the internal rotation axis of the mercapto group does not always coincide with the CS bond, 3) the dihedral angle of the mercapto group is defined around the internal rotation axis, this being 180° for the *trans* isomer and 60° for the *gauche* isomer, respectively, and 4) the methyl group is axially symmetric.

From the assumptions, the following parameters are common to the *trans* and *gauche* isomers; for the skeleton, $r$(CC), $r$(CS), for the mercapto group, $r$(SH), $\alpha$(CSH), for the methyl group, $r(\mathrm{CH_s})=r(\mathrm{CH_a})$, $\alpha$(CCH), for the methylene group, $r$(CH), $\alpha$(CCH) and the dihedral angle between the CCH and CCS planes.

They used the tilt angle of the methylene group and the angle between the CC bond and the internal rotation axis which is identical with our unperturbed $\alpha$(CCS). Their proposed structure is given in Table 6, where some of the parameter values were converted from their parameter definitions into ours. For the dihedral angle of the mercapto group for the *gauche* isomer, their value is approximately comparable to ours since the definitions are different.

We see that the proposed structure is regarded as a fairly good approximate structure for ethanethiol. In particular, the agreement for the unperturbed $\alpha$(CCS) and the tilt angle for the methylene group is surprisingly good. When the averages of our parameters for two isomers are taken, their other parameter values are in good agreement with ours within experimental error. However, they took $r$(CS) longer by *ca.* 0.01Å and $\alpha$(CSH) smaller by *ca.* 1° than our $r_s$ structural parameters.

## Dipole Moment

The dipole moment of the *trans* isomer obtained by Stark effect measurements was reported in I, discussion being given on its direction in the molecule. Schmidt and Quade[3] also reported the dipole moments both for the *trans* and *gauche* isomers. Their values of the dipole moment and its component for the *trans* isomer are in good agreement with ours. We have not carried out measurements of the dipole moment for the *gauche* isomer. However, the direction of the dipole moment can be discussed from their reported values of the dipole moment, its components, and our $r_s$ structure.

Schmidt and Quade extended their measurements of the dipole moments to the normal and four deuterated species. However, change in the dipole moment and its components by isotopic substitutions was negligible within experimental error.

They reported $\mu_a$=1.49±0.02, $\mu_b$=0.19±0.10, $\mu_c$=0.59±0.02 and $\mu_{total}$=1.61±0.05 *D* for the normal

species. It was found that the dipole moment exists along the line which makes angles of 22°35′, 83°14′, and 68°33′ with the *a*-, *b*-, and *c*-inertial axes, respectively.

From the structure, the dipole moment makes angles of 25° and 23°27′ with the CS bond and the bisector of the CSH angle, respectively. As we described in I, the dipole moments of *trans*-ethanethiol (1.560 *D*) and methanethiol (1.532 *D*) exist along lines which make angles of 28°46′ and 18°30′ with the bisector of the CSH angle in the symmetry plane inclining towards the ethyl and methyl groups, respectively. The difference in direction of the two molecules can be explained by an induced moment whose direction is from the methyl to the methylene groups in the ethyl group. When the group moment of the $CH_2SH$ part of *trans*-ethanethiol is regarded to be equal to the dipole moment of methanethiol whose direction is from the inside of the CSH angle to the apex, the induced moment of the ethyl group is found to be 0.36 *D*. The dipole moment of *gauche*-ethanethiol is calculated to be 1.77 *D* whose direction is along the line making angles of 24°4′, 82°22′, and 67°20′ with the *a*-, *b*-, and *c*-inertial axes, respectively. Though the magnitude of the calculated dipole moment is larger than the observed by about 10%, the calculated direction is in good agreement with the observed one.

## Microwave Spectra in the Excited States for *Trans* and *Gauche* Isomers

Several groups of weak spectra attributed to the excited vibrational states exist around the spectra due to the ground states of both the *trans* and *gauche* isomers.

For the *trans* isomer of the normal species, there are at least two groups of spectra whose $1_{10}\leftarrow1_{01}$ transitions are found at frequencies lower than the ground state spectra by about 410 and 480 MHz. The group of spectra whose $1_{10}\leftarrow1_{01}$ is found at 23053.85 MHz are much weaker than the other group whose $1_{10}\leftarrow1_{01}$

Table 7. Observed frequencies of *trans*-ethanethiol in excited torsional states[a] (MHz)

| Transition | SH Torsional state $v$ | $CH_3$ Torsional state $v$[b] | $\Delta v$[c] | | |
|---|---|---|---|---|---|
| $1_{10}\leftarrow1_{01}$ | 23124.59(−107) | 23053.85(−128) | −1.72(−1) | | |
| $2_{11}\leftarrow2_{02}$ | 23692.26( −51) | 23658.82( −81) | −1.75(−4) | | |
| $3_{12}\leftarrow3_{03}$ | 24562.63( 19) | 24587.58( −40) | −1.72( 6) | | |
| $4_{13}\leftarrow4_{04}$ | 25758.04( 86) | 25865.91( 14) | −1.88( 2) | | |
| $5_{14}\leftarrow5_{05}$ | 27307.60( 128) | 27526.74( 55) | −2.10(−5) | | |
| $6_{15}\leftarrow6_{06}$ | 29245.69( 71) | 29609.34( 49) | −2.27( 3) | | |
| $7_{16}\leftarrow7_{07}$ | 31611.20(−125) | 32157.45( −12) | −2.40( 8) | | |
| $1_{11}\leftarrow0_{00}$ | 32865.88( −92) | | | | |
| $2_{12}\leftarrow1_{01}$ | | 42548.71( −24) | ——[d] | | |
| $3_{03}\leftarrow2_{12}$ | 8830.71( −70) | 9089.97( −90) | 1.37( 3) | | |
| $4_{04}\leftarrow3_{13}$ | | 20207.70( −94) | 1.33( 10) | | |
| $5_{05}\leftarrow4_{14}$ | | 31521.62( 15)[e] | 1.09( 1) | | |
| $1_{01}\leftarrow0_{00}$ | 10297.88( −20) | 10339.36( −73) | | | |
| $2_{02}\leftarrow1_{01}$ | 20585.80( −14) | 20667.26( −79) | | | |
| $2_{12}\leftarrow1_{11}$ | 20039.98( 79) | 20087.45( 73) | | | |
| $2_{11}\leftarrow1_{10}$ | 21153.29( 24) | 21271.97( −57) | | | |
| $3_{03}\leftarrow2_{02}$ | 30852.79( −60) | 30971.72( −5) | | | |
| $3_{13}\leftarrow2_{12}$ | 30053.26( 87) | 30123.75( 221) | | | |
| $3_{12}\leftarrow2_{11}$ | 31723.27( 21) | 31900.71( 58) | | | |
| $A$ | 27996.23( 293) | 27928.77( 300) | $I_\alpha$(amu Å$^2$)[h] | | 3.1773 |
| $B$ | 5427.51( 36) | 5466.55( 36) | $(\lambda, \mu, \nu)$[i] | (0.7328, | 0.6805, 0) |
| $C$ | 4870.58( 34) | 4873.64( 37) | $F$(GHz)[j] | | 178.75 |
| $D_J\times10^2$[f] | 0.14 ( 390) | 2.28 ( 162) | $s$[k] | | 85.01 |
| $P_c$ (amu Å$^2$)[g] | 3.7022 | 3.4241 | $V_3$(cal/mol) | | 3260±30 |
| RMS[l] | 0.87 | 0.93 | | | |

a) Figures in parentheses indicate the difference between the observed and calculated frequencies. b) For *b*-type transitions, A component frequencies are shown. c) $\Delta\nu$ indicates the difference between A and E component frequencies. Figures in parentheses indicate differences of the observed splittings from the calculated which were computed using the listed parameters in the table. d) E component of the doublet is hidden under a strong line. e) Overlapping with a strong line with slow Stark lobes and the frequencies were obtained by measuring the Stark lobes with sine-wave Stark modulation and D. C. bias. f) Coefficient of the $[J(J+1)]^2$ term of the centrifugal distortion. g) $P_c=(I_a+I_b-I_c)/2$. For the ground state, $P_c=3.1946$ amu Å$^2$. h) Moment of intertia of the $CH_3$ group around the internal rotation axis. i) Direction cosines of the internal rotation axis in the principal inertial axes. j) $\hbar^2/2rI_\alpha$, $r=1-\lambda^2I_\alpha/I_a-\mu^2I_\alpha/I_b$. k) Reduced barrier. l) Root mean square deviation of the observed frequencies from the calculated. For the ground state, $A=28416.89(74)$, $B=5485.77(9)$, $C=4881.92(10)$, $D_J\times10^2=0.47(41)$ and RMS=0.22 MHz.

is found at 23124.59 MHz. This group of spectra exhibits doublet structures, while the other group of spectra is singlets.

Schmidt and Quade[3] also observed the spectra belonging to the stronger group and assigned them to the spectra due to the first excited mercapto torsional state. They found no spectra belonging to the weaker group. Spectra of these two groups cannot be predicted by a modified rigid rotor expression which is applied to those for the ground state. The root mean square deviations of the observed frequencies from the calculated are 0.87 and 0.93 MHz for the stronger and weaker group, respectively, while it is 0.22 MHz for the ground state. Centrifugal distortion contributions seem to be much larger for the spectra of these two groups than for those of the ground state, though the contributions cannot be determined explicitly at present because of the lack of sufficient data of the observed frequencies with different $K_{-1}$ values. Observed frequencies of the spectra are given in Table 7.

Quantities $P_c(=(I_a+I_b-I_c)/2)$ calculated from the observed rotational constants for the ground state and the two groups of the spectra are 3.1946, 3.7022, and 3.4241 amu Å$^2$, respectively. The difference in the values of the two groups and the value of the ground state $\Delta P_c(=(P_c)_{\text{excited}}-(P_c)_{\text{ground}})$ (0.5076 and 0.2295 amu Å$^2$) indicates that these groups are due to the excited states of out of plane vibrations.[10]

Schmidt and Quade measured the intensities of the stronger group spectra relative to those of the corresponding ground state spectra and concluded that the stronger group is due to the first excited state of an out of plane vibration having the frequency of 154±18 cm$^{-1}$. They presumed this vibration to be the mercapto torsion for the *trans* isomer.

For the *gauche* isomer of the normal species, two groups of weak *a*-type *R* branch spectra are also observed. Spectra of these two groups exhibit doublet structures in a similar manner to those in the ground state of the *gauche* isomer. Some of the transitions with $K_{-1}=0$ also exhibit doublet structures while the corresponding transitions in the ground state are singlets. Search for *c*-type transitions of these two groups has been unsuccessful so far. The observed frequencies are given in Table 8.

Schmidt and Quade also measured the spectra of the stronger group whose relative intensities indicate that the group is due to the excited state of a vibration having the frequency of 192±20 cm$^{-1}$. They presumed this vibration to be the mercapto torsion for the *gauche* isomer.

There are only two out of plane vibrations expected below 400 cm$^{-1}$ for each of the *trans* and *gauche* isomers, the mercapto torsion around 170 cm$^{-1}$ and the methyl torsion around 250 cm$^{-1}$. Inagaki *et al.*[11] and Manocha *et al.*[12] reported the far-infrared spectra of ethanethiol. For the mercapto torsion, they assigned a band at 158.0 cm$^{-1}$ to the 0→1 transition of the *trans* isomer and the bands at 193.0 and 191.8 cm$^{-1}$ to the $0_+\rightarrow 1_-$ and $0_-\rightarrow 1_+$ transitions, respectively, of the *gauche* isomer. The frequencies are in good agreement with those obtained from the relative intensity measurements of the microwave spectra by Schmidt and Quade for the stronger groups of the *trans* and *gauche* isomers.

For the methyl torsion, they reported only a series of bands at 247.5, 233.5, and 220.5 cm$^{-1}$ and assigned them to $v=0\rightarrow 1$, $1\rightarrow 2$, and $2\rightarrow 3$ bands of the methyl torsion, respectively.

TABLE 8. OBSERVED FREQUENCIES OF *a*-TYPE *R* BRANCH TRANSITIONS OF THE *gauche* ISOMER IN THE GROUND AND FIRST EXCITED TORSIONAL STATES[a] (MHz)

| Transition[b] | Ground state | SH excited state | $CH_3$ excited state |
|---|---|---|---|
| $1_{01}\leftarrow 0_{00}{}^{++}_{--}$ | 10141.07( 11) | 10133.84( 201) | 10116.10( 11) |
| $2_{02}\leftarrow 1_{01}{}^{++}_{--}$ | 20275.47( 5) | 20260.60( 166)<br>20261.70 | 20225.79( 2) |
| $2_{12}\leftarrow 1_{11}{}^{++}_{--}$ | 19832.99( 17)<br>19836.33 | 19812.60( 189)<br>19809.92 | 19790.24( 24)<br>19784.31 |
| $2_{11}\leftarrow 1_{10}{}^{++}_{--}$ | 20727.77<br>20730.83(−18) | 20718.60<br>20714.08(−254) | 20679.91<br>20674.00( 4) |
| $3_{03}\leftarrow 2_{02}{}^{++}_{--}$ | 30396.99( 0) | 30376.34( −25)<br>30374.29 | 30323.17( 4)<br>30322.86 |
| $3_{13}\leftarrow 2_{12}{}^{++}_{--}$ | 29745.06(−14)<br>29736.75 | 29711.10(−203)<br>29714.60 | 29680.95(−20)<br>29685.13 |
| $3_{12}\leftarrow 2_{11}{}^{++}_{--}$ | 31101.19<br>31092.82( 9) | 31067.98<br>31072.88( 93) | 31002.77<br>31006.96( −7) |
| $B$[c] | 5295.03( 16) | 5292.39( 228) | 5278.99( 17) |
| $C$[c] | 4845.93( 16) | 4839.44( 225) | 4837.01( 16) |
| RMS[d] | 0.16 | 2.34 | 0.17 |

a) Figures in parentheses indicate the differences between the observed and calculated frequencies. b) ++ indicates the transition from the + state to the + state. For the first excited SH torsional state, tentative assignments are given in the table for the ++ and −− components of the doublets. c) Since the *gauche* isomer is very close to the prolate symmetric top, *a*-type transition frequencies can be expressed only by *B* and *C* rotational constants. Figures in parentheses indicate 99% reliability intervals calculated from 2.5 times the standard deviation. d) Root mean square deviation of the observed frequencies from the calculated. For the SH and $CH_3$ excited torsional states, RMS is 3.01 and 5.04 MHz, respectively if the choice of the components of the observed frequencies is reverse.

The doublet structures observed for the spectra belonging to the weaker group of the *trans* isomer indicate that the group is due to the first excited state of the methyl torsion. For the *gauche* isomer, the weaker group of the spectra may also be due to the first excited methyl torsional state, though there is no definite evidence for the assignment of the group.

For the methyl excited torsional state for the *gauche* isomer, components of doublets predictable by a rigid rotor expression are reverse in frequency to those for the ground state (Table 8). This is understood qualitatively as follows.

For the methyl excited torsional state, smallness of the splittings of the transitions with $K_{-1}=0$ indicates that the rotational constants of the + and − states are nearly equal in a similar manner to the ground state. However, the energy difference of the + and − states (estimated to be about 1300 MHz) seems to be much smaller than that for the ground state (determined to be 1750 MHz). This is obvious from the fact that the splittings of $J=1\rightarrow2$ are larger than those of $J=2\rightarrow3$, the reverse of the case for the ground state.

Schematic energy and transition diagrams for cases of no interactions, and ground and methyl excited torsional states are shown in Fig. 3. If there are no interactions between the + and − states, *a*-type transitions of both states have the same frequencies. For the ground state the interaction occurs strongly between the accidentally degenerate levels which are $K_{-1}=1$ levels for low $J$. Since the $2_{11}^{+}$ level is lower than the $2_{12}^{-}$ level, both levels are pushed down and up, respectively, by an amount of $\Delta\nu_2$. For the degenerate case of $(1_{10}^{+}, 1_{11}^{-})$ and $(3_{12}^{+}, 3_{13}^{-})$, $1_{10}^{+}$ and $1_{11}^{-}$ levels shift to lower and higher energy by an amount of $\Delta\nu_1$, and $3_{12}^{+}$ and $3_{13}^{-}$ levels are pushed up and down by an amount of $\Delta\nu_3$, respectively, since $1_{10}^{+}$ and $3_{13}^{-}$ levels are lower than the $1_{11}^{-}$ and $3_{12}^{+}$ levels, respectively. Thus the frequencies of the transitions concerned with $K_{-1}=1$ levels are

$$\left.\begin{aligned}\nu(1_{10}^{+}\rightarrow2_{11}^{+}) &= \nu_2+\Delta\nu_1-\Delta\nu_2,\\ \nu(1_{11}^{-}\rightarrow2_{12}^{-}) &= \nu_1-\Delta\nu_1+\Delta\nu_2,\\ \nu(2_{11}^{+}\rightarrow3_{12}^{+}) &= \nu_4+\Delta\nu_2+\Delta\nu_3,\\ \nu(2_{12}^{-}\rightarrow3_{13}^{-}) &= \nu_3-\Delta\nu_2-\Delta\nu_3,\end{aligned}\right\}\quad(9)$$

where $\nu_1$, $\nu_2$, $\nu_3$, and $\nu_4$ indicate the unperturbed frequencies of the corresponding transitions, whereas $\nu(1_{11}^{+}\rightarrow2_{12}^{+})$, $\nu(1_{10}^{-}\rightarrow2_{11}^{-})$, $\nu(2_{12}^{+}\rightarrow3_{13}^{+})$, and $\nu(2_{11}^{-}\rightarrow3_{12}^{-})$ are nearly unperturbed frequencies, since the levels are not in degeneracy.

On the other hand, for the methyl excited torsional state, since the $2_{11}^{+}$ level is higher than the $2_{12}^{-}$ level, the $2_{11}^{+}$ and $2_{12}^{-}$ levels are pushed up and down by an amount of $\Delta\nu_2$ as shown in Fig. 3(C). The directions of these shifts are the reverse of those for the case of the ground state. The frequencies of the transitions which are strongly affected by the interactions are

$$\left.\begin{aligned}\nu(1_{10}^{+}\rightarrow2_{11}^{+}) &= \nu_2+\Delta\nu_1+\Delta\nu_2,\\ \nu(1_{11}^{-}\rightarrow2_{12}^{-}) &= \nu_1-\Delta\nu_1-\Delta\nu_2,\\ \nu(2_{11}^{+}\rightarrow3_{12}^{+}) &= \nu_4-\Delta\nu_2+\Delta\nu_3,\\ \nu(2_{12}^{-}\rightarrow3_{13}^{-}) &= \nu_3+\Delta\nu_2-\Delta\nu_3.\end{aligned}\right\}\quad(10)$$

Since the $(2_{11}^{+}, 2_{12}^{-})$ couple is more degenerate than the $(3_{12}^{+}, 3_{13}^{-})$ couple, $\Delta\nu_2>\Delta\nu_3$, and then $\nu(2_{11}^{+}\rightarrow3_{12}^{+})$ is lower than $\nu(2_{11}^{-}\rightarrow3_{13}^{-})$ which is nearly equal to $\nu_4$.

For the mercapto excited torsional state, splittings of the transitions with $K_{-1}=0$ are not small and the differences in the rotational constants of the + and − states are not negligible (Table 8).

According to the theoretical calculation, the rotational constants of the + and − states are nearly equal to each other within 0.1 MHz for the ground state, while they differ by *ca.* 5 MHz for the first excited mercapto torsional state. The observed results are in line with the calculated results. Though the coefficients of the cross terms $D_{\pm}$ and $E_{\pm}$ remain nearly unchanged between the ground and excited states, coefficients $N$ and $Q$ which correspond to the so-called Coriolis terms become about 25 times larger for the excited state than those for the ground state.

We see from Table 8 that the observed frequencies of *a*-type transitions for the mercapto excited torsional state cannot be fitted satisfactorily with a rigid rotor expression whatever choice of components of the doublets is used. This might be explained by the above results of the theoretical calculation.

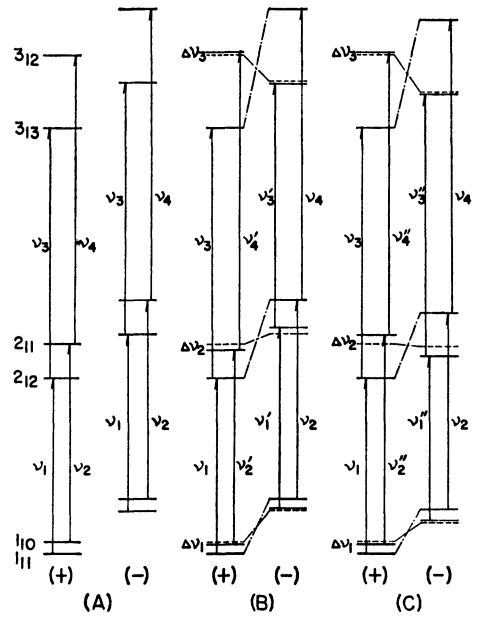


Fig. 3. Schematic energy and transition diagrams for the cases of (A) no interactions, (B) ground state and (C) methyl excited torsional state for the normal species.
Solid and dotted lines indicate perturbed and unperturbed levels, respectively.
For (B), $\nu_1'=\nu_1-\Delta\nu_1+\Delta\nu_2$, $\nu_2'=\nu_2+\Delta\nu_1-\Delta\nu_2$, $\nu_3'=\nu_3-\Delta\nu_2-\Delta\nu_3$, and $\nu_4'=\nu_4+\Delta\nu_2+\Delta\nu_3$, for (C), $\nu_1''=\nu_1-\Delta\nu_1-\Delta\nu_2$, $\nu_2''=\nu_2+\Delta\nu_1+\Delta\nu_2$, $\nu_3''=\nu_3+\Delta\nu_2-\Delta\nu_3$, and $\nu_4''=\nu_4-\Delta\nu_2+\Delta\nu_3$. See text.

## Internal Rotation of the Methyl Group

As is shown in Table 7, from the observed splittings of the spectra attributed to the first excited methyl torsional state of the *trans* isomer, the barrier to internal rotation of the methyl group was determined to be $V_3=3260\pm30$ cal/mol by the principal axis method

neglecting the coupling effect of the mercapto internal rotation.

Schmidt and Quade[3] also reported the $V_3$ value as 3306±86 cal/mol which was obtained from very small splittings of high $J$, high $K_{-1}$ transitions found in the ground state of the *trans* isomer. Their value is essentially identical with ours within experimental error.

Manocha *et al.*[12] observed only one weak series of far-infrared bands at the higher frequency wing of the strong mercapto torsion band due to the *gauche* isomer. They assigned them to the $v=0\rightarrow1$, $1\rightarrow2$, and $2\rightarrow3$ bands of the methyl torsion, though they did not confirm to which isomer these bands belong. From these bands, the barrier was calculated to be $V_3=3886\pm60$ and $V_6=-69\pm23$ cal/mol.

According to the relative intensity measurements of the microwave spectra by Schmidt and Quade, the *gauche* isomer is more stable by 406±43 cal/mol than the *trans* isomer so that populations of the *trans* and *gauche* isomers are in the ratio of *ca.* 1 : 4 at room temperature where the far-infrared spectra were observed. The barrier obtained from the far-infrared data probably belongs to the *gauche* isomer. The barrier of the methyl internal rotation for the *trans* isomer is lower by *ca.* 630 cal/mol than that for the *gauche* isomer.

Hirota[13] reported the barriers for the *trans* and *gauche* isomers of propyl fluoride which are 2690 and 2865 cal/mol, respectively. For this molecule, the barrier for the *trans* isomer is also lower by 175 cal/mol than that for the *gauche* isomer but change of the barrier is not so prominent as for ethanethiol.

Barriers to internal rotation of the $CH_3$–C group for a series of molecules; ethyl chloride,[14] ethyl bromide,[15] ethyl fluoride,[16] propane,[17] *trans*-ethyl methyl ether,[18] and *trans*-ethanol,[19] were reported to be 3685, 3684, 3330, 3325, 3300, and 3323 cal/mol, respectively. The barrier of *gauche*-ethanethiol is the highest among these molecules, while that of *trans*-ethanethiol is the lowest.

## Internal Rotation of the Mercapto Group

The barrier to the mercapto internal rotation was determined using the Hamiltonian (1b) with the first three terms with the coefficients $V_1$, $V_2$, and $V_3$ of the potential function. Coefficients $\mu_\alpha^{(n)}$ of the kinetic terms were calculated on the basis of the $r_s$ structure including the tilt angle. The first three terms of the kinetic terms were taken into consideration, though the coefficients $\mu_\alpha^{(1)}$ and $\mu_\alpha^{(2)}$ of the second and third terms were much smaller than that of the first term, $\mu_\alpha^{(0)}$.

The energy matrix was constructed from the Hamiltonian (1b) and the basis functions were chosen as $\{(1/\sqrt{2\pi}), (1/\sqrt{\pi})\cos\alpha,\cdots, (1/\sqrt{\pi})\cos 30\alpha\}$ for the symmetric states and $\{(1/\sqrt{\pi})\sin\alpha,\cdots, (1/\sqrt{\pi})\sin 30\alpha\}$ for the antisymmetric states. The torsional energy levels were obtained by a direct diagonalization of the energy matrix. A least squares analysis was carried out taking $V_1$, $V_2$, and $V_3$ as parameters in order to reproduce the energy differences of the + and − states of the *gauche* isomer obtained from the microwave spectra and those obtained from seven observed mercapto torsional frequencies of the *trans* and the *gauche* isomers reported by Manocha *et al.*[12] both for the normal and $CH_3CH_2SD$ species. The results are given in Table 9 and the resulting potential curve together with the energy levels in Fig. 4. The results reported by Schmidt and Quade and by Manocha *et al.* are also given in Table 9 for the sake of comparison.

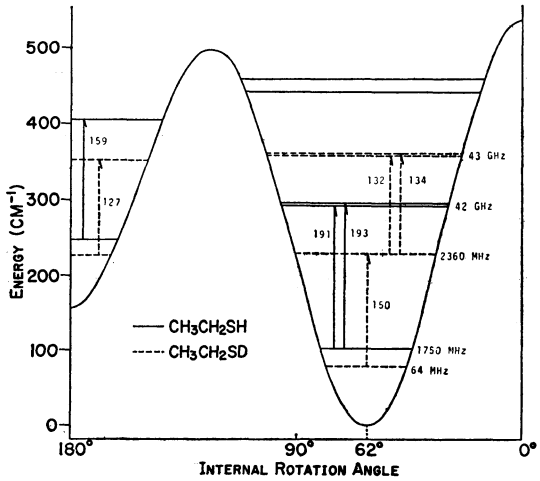


Fig. 4. Potential curve, energy levels and transition frequencies of mercapto internal rotation.

Since the assumed structure used by Schmidt and Quade is close to our $r_s$ structrue, the $\mu_\alpha^{(n)}$ values do not differ much between their calculation and ours. However, they disregarded the $\mu_\alpha^{(1)}$ and $\mu_\alpha^{(2)}$ terms since they were much smaller than the $\mu_\alpha^{(0)}$ term, while we included these terms in our calculation.

In order to know the influence of these terms, a calculation was made using our data neglecting these terms. It was found that the influence is negligible for the barrier values. The differences in the barrier values in our results and those by Schmidt and Quade are considered to be due to the data used in the calculations. Since their data obtained mainly from the intensity measurements have relatively large uncertainties, our results may be more reliable.

The energy differences used by us and by Manocha *et al.* are the same except for those of $g^0_+-g^0_-$ which were added to the data in our calculation. On the other hand, their assumed structure differs a great deal from our $r_s$ structure. Actually, they used the $\mu_\alpha^{(n)}$ values calculated by Inagaki *et al.*[11] who obtained these coefficient values from a model structure. The structure is; $r(CS)=1.81$, $r(CC)=1.53$, $r(CH)=1.095$, and $r(SH)=1.329$ Å, $\alpha(CSH)=100°18'$ and other angles =tetrahedral. Not only do their structural parameters differ a great deal from the $r_s$ structural parameters but the tilt angle was not taken into consideration. The $\mu_\alpha^{(n)}$ values of their calculations and ours greatly differ. The $\mu_\alpha^{(1)}$ and $\mu_\alpha^{(2)}$ values are much larger than ours. Furthermore, using four energy differences for the $CH_3CH_2SD$ species, they could determine not only the $V_1$, $V_2$, and $V_3$ values but also the $V_6$ value which was neglected in our calculation.

For a comparison of our results with theirs, trial calculations were carried out with several different choices of $\mu_\alpha^{(n)}$ values and the data. It can be concluded

TABLE 9. RESULTS FOR THE MERCAPTO INTERNAL ROTATION

| Barrier (cal/mol)[a] | Present work | | Schmidt and Quade | | Manocha *et al.* | |
|---|---|---|---|---|---|---|
| $V_1$ | −207 (67) | | −186 | | −123 (63) | |
| $V_2$ | −386 (27) | | −386 | | −392 (20) | |
| $V_3$ | 1305 (20) | | 1258 | | 1355 ( 6) | |
| $V_6$ | —— | | —— | | −37 ( 3) | |
| Kinetic coef. ($cm^{-1}$) | $CH_3CH_2SH$ | $CH_3CH_2SD$ | $CH_3CH_2SH$ | $CH_3CH_2SD$ | $CH_3CH_2SH$[b] | $CH_3CH_2SD$[b] |
| $\mu_\alpha^{(0)}$ | 10.870 | 6.091 | 10.78 | 6.02 | 10.9735 | 6.0756 |
| $\mu_\alpha^{(1)}$ | −0.011 | −0.046 | —— | —— | −0.1617 | −0.1601 |
| $\mu_\alpha^{(2)}$ | 0.020 | 0.006 | —— | —— | 0.0362 | 0.0424 |
| $\mu_\alpha^{(3)}$ | —— | —— | —— | —— | −0.0017 | −0.0034 |
| $\mu_\alpha^{(4)}$ | —— | —— | —— | —— | 0.0002 | 0.0004 |
| Energy dif. ($cm^{-1}$)[c] | | | | | | |
| $g0_+ - g0_-$ | 0.05851 (−3) (p) | 0.00234 (20) (p) | 0.058 (−2) (q) | 0.0023 ( 3) (q) | 0.05851 (318) (p)[e] | 0.00234 (40) (p)[e] |
| $t0 - t1$ | 158.0 (−15) (r) | 125.0 (−24) (r) | 154.0 ( 0) (q) | —— | 158.0 (−25) (r)[e] | 125.0 (0) (r) |
| $g0_+ - g1_-$ | 193.0 ( 2) (r) | 148.5 (−15) (r) | 192.0 ( 50) (q) | 147.0 ( 10) (q) | 193.0 ( −1) (r)[e] | 148.5 (0) (r) |
| $g0_- - g1_+$ | 191.8 ( 4) (r) | | | | 191.8 ( 0) (r)[e] | |
| $g1_+ - g2_-$ | —— | 135.1 ( 15) (r) | —— | —— | —— | 135.1 (0) (r) |
| $g1_- - g2_+$ | —— | 134.1 ( 19) (r) | —— | —— | —— | 134.1 (0) (r) |
| $t0 - g0_\pm$ | 142.0 (−21) (q)[d] | 138.0 (−90) (q)[d] | 142.0 ( 40) (q) | 138.0 (−40) (q) | —— | —— |

a) Figures in parentheses indicate the uncertainties attached to the last significant figures. b) Quoted from the paper by Inagaki *et al.* (Ref. 11). Manocha *et al.* used these values for the $CH_3CH_2SD$ species in their determination of the barrier values. c) $g0_+ - g0_-$ indicates the energy difference between the $0_+$ and $0_-$ levels for the *gauche* isomer. Figures in parentheses indicate the deviations of the observed values from the calculated and symbols in parentheses indicate the method used for obtaining the data quoted, that is, (p); the splitting analysis of the microwave spectra by the present authors, (q); the splitting analysis and the relative intensity measurements of the microwave spectra by Schmidt and Quade (Ref. 3); (r); the far-infrared spectra by Manocha *et al.* (Ref. 12). d) These data were not included in a least squares analysis since they were considered to have relatively large uncertainties. e) These data were not used by Manocha *et al.* in the determination of the $V$ values. Deviations of the observed values from the calculated were not shown in their paper but we calculated them using their parameters.

that 1) discrepancies found in the barrier values obtained by the present authors and by Manocha *et al.* arise form the structure used in the calculations and 2) the $V_6$ value cannot be determined in sufficient accuracy if the $\mu_\alpha^{(n)}$ values based on the $r_s$ structure are used in the calculation.

**References**

1) M. Hayashi, H. Imaishi, K. Ohno, and H. Murata, *Bull. Chem. Soc. Jpn.*, **44**, 872 (1971).
2) M. Hayashi, H. Imaishi, and K. Kuwada, *Bull. Chem. Soc. Jpn.*, **47**, 2382 (1974).
3) R. E. Schmidt and C. R. Quade, *J. Chem. Phys.*, **62**, 2864 (1975).
4) See also, M. Hayashi, J. Nakagawa, and K. Kuwada, *Chem. Lett.*, **1975**, 1267.
5) A. Murray, III. and D. L. Williams, "Organic Syntheses with Isotopes," Part II, Interscience, New York (1958), pp. 1340, 1341.
6) C. R. Quade and C. C. Lin, *J. Chem. Phys.*, **38**, 540 (1963); J. V. Knopp and C. R. Quade, *ibid.*, **48**, 3317 (1968).
7) D. R. Lide, Jr., *J. Chem. Phys.*, **33**, 1514 (1961).
8) T. Kojima and T. Nishikawa, *J. Phys. Soc. Jpn.*, **12**, 680 (1957); T. Kojima, *ibid.*, **15**, 1284 (1960).
9) L. Pierce and M. Hayashi, *J. Chem. Phys.*, **35**, 479 (1961).
10) D. R. Herschbach and V. W. Laurie, *J. Chem. Phys.*, **40**, 3142 (1964).
11) F. Inagaki, I. Harada, and T. Shimanouchi, *J. Mol. Spectrosc.*, **46**, 381 (1973).
12) A. S. Manocha, W. G. Fateley, and T. Shimanouchi, *J. Phys. Chem.*, **77**, 1977 (1973).
13) E. Hirota, *J. Chem. Phys.*, **37**, 283 (1962).
14) R. H. Schwendeman and G. D. Jacobs, *J. Chem. Phys.*, **36**, 1245 (1962).
15) C. Flanagan and L. Pierce, *J. Chem. Phys.*, **38**, 2963 (1963).
16) B. Bak, S. Detoni, L. Hansen-Nygaard, J. Tormod Nielsen, and J. Rastrup-Andersen, *Spectrochim. Acta*, **16**, 376 (1960).
17) E. Hirota, C. Matsumura, and Y. Morino, *Bull. Chem. Soc. Jpn.*, **40**, 1124 (1967).
18) M. Hayashi and K. Kuwada, *J. Mol. Struct.*, **28**, 147 (1975).
19) J. P. Culot, Austin Symp. Gas Phase Mol. Struct., (1972), T8.